Calculation of the Tafel Plot for H_2 Oxidation on Pt(100) from Potential-Dependent Activation Energies

Alfred B. Anderson* and Yu Cai

Chemistry Department, Case Western Reserve University, Cleveland, Ohio 44106

Received: August 23, 2004; In Final Form: November 5, 2004

Quantum mechanically determined electrode potential dependent activation energies for hydronium ion discharge over Pt−H (Heyrovsky reaction) and the reverse reaction have been used to predict Tafel plots. The calculated Tafel plot for H_2 oxidation is similar in shape to an experimental plot from the literature for a Pt(100) electrode and will overlap it when an appropriate preexponential factor is chosen in the Arrhenius expression. This provides strong theoretical support for the first electron-transfer step being rate limiting during H_2 oxidation over the potential range 0 to 0.15 V, and the second electron-transfer step being rate limiting during H_2 evolution over this electrode. The exchange current density is determined from the calculated oxidation and reduction currents and is found to overestimate experiment primarily because the predicted activation energy at the reversible potential underestimates the experimental value. This study illustrates that curvature in nonlinear Tafel plots may stem from the potential dependence of the activation energies or transfer coefficients as well as diffusion and concentration gradient effects. The observed current density and its increase, leveling off, and then decrease at potentials greater than the activation energy-controlled region are attributed to removal of under potential deposited H, passing through the double layer region, and then site blocking by water and its oxidation product OH(ads).

Introduction

On the basis of the shapes of the Tafel plots (electrode potential vs log current density) for hydrogen oxidation on the (111), (110), and (100) surfaces of platinum Markovic, Grgur, and Ross proposed that H_2 is oxidized by the Volmer−Heyrovsky mechanism on Pt(100).[1] For the reduction reaction, this mechanism has as its first step hydronium ion discharge over a bare surface site to form surface Pt−H, which is called the Volmer reaction, eq 1:

$$\mathrm{Pt} + \mathrm{H^+(aq)} + \mathrm{e^-} \rightarrow \mathrm{Pt{-}H} \qquad (1)$$

This is followed by the discharge of a second hydronium ion on this H to yield H_2, which is called the Heyrovsky reaction and is presumed to be rate limiting:

$$\mathrm{Pt{-}H} + \mathrm{H^+(aq)} + \mathrm{e^-} \rightarrow \mathrm{Pt} + \mathrm{H_2} \qquad (2)$$

The oxidation reaction is the reverse of this, with H_2 coordinating to a bare surface Pt site, followed by two oxidation steps generating two hydronium ions. Over the Pt(110) surface the Volmer−Tafel mechanism was proposed on the basis of the Tafel plots.[1] For the reduction reaction, this mechanism also has as its first step the discharge of a hydronium ion on a bare Pt site but for the second step two such chemisorbed H atoms combine to make H_2, in what is presumed to be the rate-limiting step:

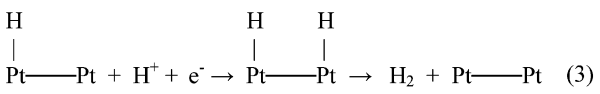

(3)

The oxidation reaction is the reverse of this. The authors of ref 1 could not distinguish between the two mechanisms in the case of Pt(111).

In general, for single step electrode reactions the kinetic current density, i_k, at a given electrode potential, U, is, in the high overpotential region, given by an Arrhenius expression:

$$i_k = A(U)\exp(-E_a(U)/RT) \qquad (4)$$

where the preexponential factor A is proportional to the concentration of species undergoing oxidation or reduction, the number of active sites per unit area, the frequency factor, and the Faraday constant, and it may vary with temperature and potential due to adsorption of electrolyte components, reaction intermediates, and surface restructuring. E_a is the activation energy for the oxidation or reduction reaction and T is the temperature of the system. In the low overpotential region both forward and reverse reactions contribute and the total current density is

$$i_k = |i_{kox} - i_{kred}| = A(U)|\exp(-E_a^{ox}(U)/RT) - \exp(-E_a^{red}(U)/RT)| \qquad (5)$$

where i_{kox} and i_{kred} stand for oxidation and reduction kinetic current densities. When it is assumed that $A(U)$ is constant and that the activation energies are linear in the oxidation overpotential, which is defined as $\eta = U - U^\circ$, this becomes the widely used Butler−Volmer equation:

$$i_k = i_o[\exp(\beta\eta F/RT) - \exp(-(1-\beta)\eta F/RT)] \qquad (6)$$

where i_o is the exchange current density and β is the symmetry factor.

* Corresponding author. E-mail: aba@po.cwru.edu. Phone: 216-368-5044. Fax: 216-368-3006.

10.1021/jp046194c CCC: $27.50 © 2004 American Chemical Society
Published on Web 11/24/2004

Tafel plots are graphs relating the log of the measured kinetic current to overpotential. They are often linear in the high overpotential regions and when this is true the kinetic current is given by

$$i_k = i_o[\exp(\alpha_a \eta F/RT) - \exp(-\alpha_c \eta F/RT)] \quad (7)$$

where α_a and α_c are called, respectively, the anodic and cathodic transfer coefficients. This phenomenological equation is assumed in analyses of measured kinetic currents, including multistep electron-transfer reactions when α_a is constant so that there is a well-defined Tafel slope in the high oxidation overpotential region. In this case, one has

$$\log i_k = \log i_o + \alpha_a \eta F/RT \quad (8)$$

and at the reversible potential, when $\eta = 0$, the exchange current density equals the measured kinetic current. This is obtained by linear extrapolation in the Tafel plot. However, the graph may not be linear, so that the Tafel slope and i_o become ill defined. Such nonlinear behavior can arise for a variety of reasons, including the potential dependence of the transfer coefficient, which is generally unknown, and diffusion and concentration gradient effects.

A second method for determining exchange current densities makes use of the relation

$$\alpha_a + \alpha_c = n/\nu \quad (9)$$

where n is the number of electrons transferred in the reaction, $n = 2$ for the hydrogen oxidation or formation reaction, and ν is the stoichiometric number, which is the number of times the rate determining step must occur; $\nu = 1$ for the mechanisms considered here.[2]

When eq 9 with these parameters is substituted in eq 7 and the exponential terms are expanded in the low over potential linear "micropolarization" range, a formula for exchange current density is obtained that is independent of the values of the transfer coefficients:

$$i_o = (RT/F)\Delta i/2\eta \quad (10)$$

The authors of ref 1 used both Tafel plot extrapolations and the slopes in the micropolarization regions to determine exchange current densities for the three platinum surfaces and, assuming that $\nu = 1$ for all three electrode surfaces, the two approaches were in good agreement.

We have recently calculated electrode potential-dependent activation energies for Pt−H formation and oxidation, the Volmer reaction, and for H_2 formation by hydronium ion discharge over Pt−H and its oxidation, the Heyrovsky reaction. These calculations employed a single Pt site and no coverage dependence in what is referred to as a local reaction site model and the system was treated as an open one, with the electron tunneling in or out of it when its electron affinity or ionization potential matched the thermodynamic work function, or potential, of the electrode. The electrode is not explicitly included in the calculations.[3−6] This tunneling concept was proposed by Gurney[7] and is basic to the Marcus theory for outer sphere reactions.[8] The approach used here treats the electron transfer to or from the local reaction center as an outer sphere reaction and it is sensible for bond breaking and bond forming electrochemical reactions in molecules when the bonds are localized chemical bonds. A single Pt atom was used to represent the site, and reaction energies were corrected to take into account the stronger Pt−H bond compared to the H chemisorption bond to the Pt surface.[4,5]

The use of the local reaction site model allows control of the potential of the electron source or sink, that is, the electrode potential, over a wide range and the electron tunnels from or to the bonds that are being rearranged by the reaction. Large cluster models will prevent this approach from working because their electron affinities and ionization potentials converge toward the surface work function. This destroys the potential control provided by the theory because the clusters themselves become the source or sink for electron-transfer rather than the reaction site with the bonds being made or broken there. Controlling the potential of an extended system would require the full treatment of surface charging, the double layer structure, and the bulk electrolyte, an enormous challenge.

The activation energy for the Heyrovsky step at the calculated reversible potential was 0.076 eV, and the experimentally determined apparent activation energy for the overall two-electron H_2 oxidation Pt(100) was 0.12 eV, as determined from an Arrhenius plot of exchange current densities. It is of interest whether the theoretically determined potential-dependent activation energies from ref 6 for the Heyrovsky reaction are capable in themselves, when substituted into eq 5, of predicting the observed Tafel plot over the reported 150 mV range, without including any potential or coverage dependence in *A*. A satisfactory fit would imply (i) the rate determining step is the Heyrovsky step and (ii) a nearly constant concentration of active sites exists on the electrode surface over this potential range. We note that the experimental reference electrode employed a salt bridge, which can cause inaccuracies is potential measurement that can, as Conway and Wilkinson have shown, be temperature dependent.[9] Any resulting corrections to activation energies evaluated from exchange current densities are presently not known but have been assumed to be small in the literature.

Theoretical Approach

Our theoretical model has been presented in detail in refs 3−6 and references therein. MP2 calculations were performed using Gaussian 94 software with the 6-31G** basis set for light atoms and a core pseudopotential and Los Alamos double-ζ basis set LANL2DZ for Pt.[10] The hydronium ion (H_3O^+) used in the calculations has two water molecules hydrogen bonded to it and one H available to transfer as the reaction proton. A potential term is added to the Hamiltonian corresponding to a Madelung potential representing ~0.1 M monoprotic acid with hydronium ions and anions in a regular array above the electrode surface. The electron-transfer transition state at each potential is calculated as the lowest energy point on a surface of constant electron affinity, EA (for reduction) or ionization potential, IP (for oxidation) where

$$\text{EA or IP} = (4.6 + U/\text{V})\ \text{eV} \quad (11)$$

Constrained variation theory is used.[11] The 4.6 in eq 11 is the work function of the standard hydrogen electrode in eV.[12] The reaction model for the Heyrovsky reaction is

$$\text{Pt}-\text{H}\cdots\text{H}^+-\text{OH}_2(\text{OH}_2)_2 + \text{e}^-(U) \leftrightarrow \text{Pt}\cdots\text{H}-\text{H}\cdots\text{OH}_2(\text{OH}_2)_2 \quad (12)$$

Equation 12 makes clear the bond rearrangement associated with the reduction and oxidation reaction, and at the transition states the structures of the oxidized and reduced systems are the same.

Results and Discussion

The calculated activation energies for oxidation and reduction in eq 12 are in Figure 1.

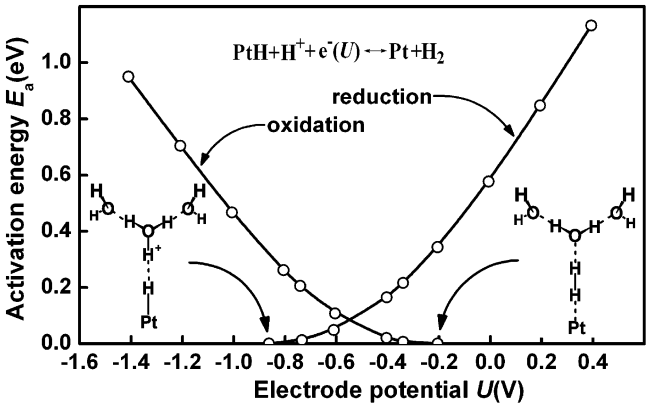

Figure 1. Calculated activation energies as functions of electrode potential for the Heyrovsky mechanism.

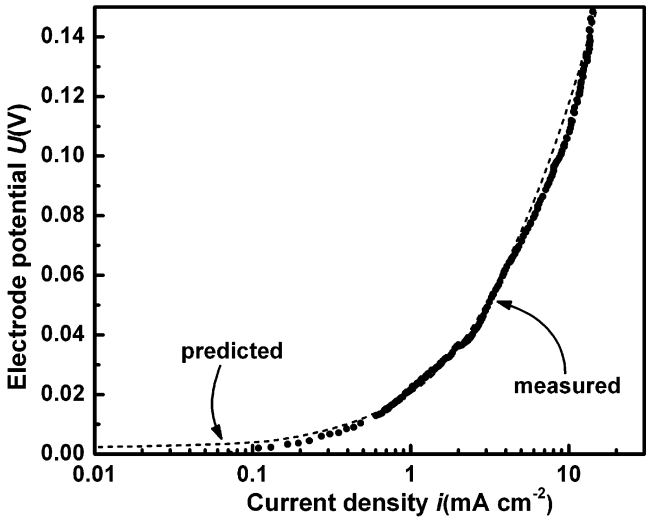

Figure 2. Predicted Tafel plot from substituting activation energies from Figure 1 for the first step in H_2 oxidation by the Heyrovsky mechanism into eq 5 (dashed line) compared to measurements at 274 K for the overall two-electron oxidation of H_2 from ref 1 (dots). The current densities are kinetic current densities with the subscript k omitted in the label.

More points have been added compared to the published curves in ref 6 in order to ensure well-defined Tafel plot predictions. Substitution of these energies into eq 5 produces a smooth curve in the log i_k vs U plot for oxidation, and when the constant value 33 is chosen for the preexponential factor, the curve fits the measured Tafel data at 274 K (from ref 1) for oxidation on the Pt(100) electrode, as shown in Figure 2. For this reaction A includes a factor 2 for two electrons transferred. From one perspective the whole Tafel curve for H_2 oxidation can be viewed as curved, or it can be viewed as made of two linear regions, as was assumed previously.[1]

Attempts to fit the theoretical curve to the Tafel data from ref 1 for H_2 oxidation on the (110) and (111) electrodes by varying the preexponential A factor did not succeed. This is consistent with the Volmer−Heyrovsky mechanism not applying to these electrode surfaces. As pointed out in ref 1, the measured 28 mV/decade Tafel slope for the (110) surface is consistent with the Tafel−Volmer mechanism with H atom recombination or H_2 dissociation being the rate determining step on this surface. For the (111) electrode the calculated curve could fit the experimental Tafel plot only up to 0.07 V, which is consistent with the ambiguity discussed in ref 2.

Figure 3 presents the oxidation and reduction components of eq 5 along with an extended plot of experimental data beyond

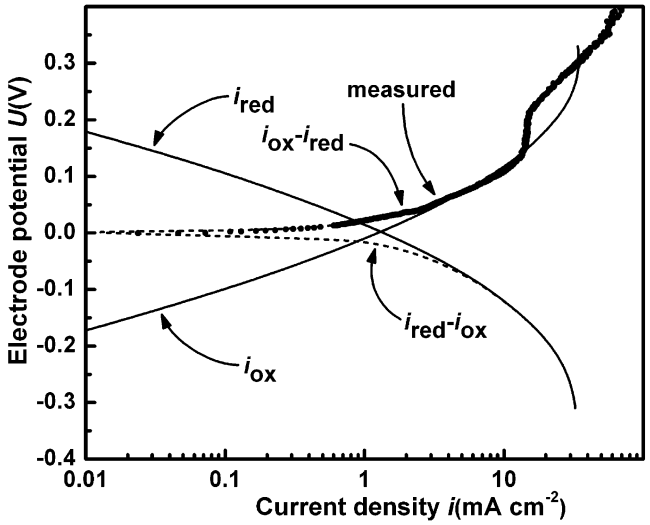

Figure 3. Curves labeled i_{ox} and i_{red} are the oxidation and reduction components of the total predicted current densities for oxidation and reduction that are indicated by dashed lines. The measured points at 274 K are dots as in Figure 1, and additional data at higher potentials are included. The current densities are kinetic current densities with the subscript k omitted in the labels.

the previously published 0.15 V limit. The reduction curve in Figure 3 crosses the oxidation curve at the exchange current density, where i_{kox} and i_{kred} in eq 5 are equal, at 0 V. This crossing occurs in the high overpotential region. The predicted value is 1.3 mA cm^{-2} compared to the measured 0.36 mA cm^{-2} on the basis of extrapolation of the Tafel plot and on the slope in the micropolarization region.[2] Essentially the same value, 1.2 mA cm^{-2} is obtained using eq 4 with $A = 33$, $E_a(0) = 0.076$ eV, and $T = 274$ K, the difference being due to rounding A to 33. When the activation energies are expanded in a second-order Taylor series around the reversible potential and the linear term is used to generate a new Figure 3, the slope is between the two linear regions in the experimental Tafel plot crossing point and i_o decreases slightly to 1.0 mA cm^{-2}, and when the second order term is added, the predicted curves are essentially the same as in Figures 2 and 3 and the predicted i_o is again 1.3 mA cm^{-2}. It is not surprising that the lower parts of the activation energy curves in Figure 1 can be well fit by quadratic expansions. However, predicted exchange current density is too high and this overestimation can be related in part to the underestimation of the activation energy at 0 V, 0.076 eV calculated vs 0.12 eV from measurement reported in ref 1, and in part to the slopes of the activation energies in Figure 1 being too shallow. These influences can be examined. Assuming that i_o is proportional to the exponential of the activation energy divided by RT, i_o becomes 0.20 mA cm^{-2} when E_a is increased to 0.12 eV. This value is too small; however, the exponential terms in eqs 5 and 6 will be affected and a new fitting would be required, with a constant smaller than 33, and the crossing point in Figure 3 would have to be calculated. It is notable that platinum is an excellent catalyst for hydrogen reactions, which is why the activation energy is very small, not much larger than the ∼1 kcal mol^{-1} uncertainty of the calculated MP2 results. Consequently, the predicted $E_a(0)$ is uncertain due to calculational as well as modeling effects.

Figure 3 shows a sharp rise in the theoretically predicted Tafel graph at about 0.25 V and this is due to reaching the potential of the oxidation precursor, for which the activation energy for oxidation is zero. The experimental curve shows a sharp increase in current density at about 0.15 V, which could be due to

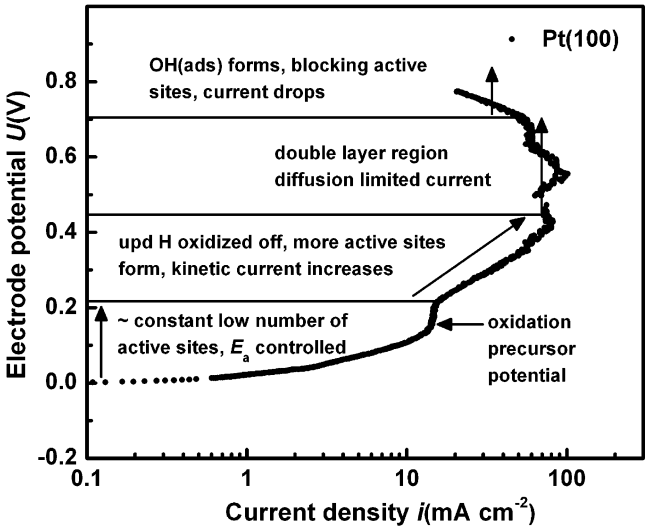

Figure 4. As in Figure 3 for plot of all data from the authors of ref 1 with proposed interpretations for the kinetic current in different potential regions.

reaching the potential of the oxidation precursor. If so, the 0.1 V discrepancy is attributable to simplicity of the modeling procedure. At just beyond 0.2 V the current begins to rise again and this suggests the possibility that the oxidation of underpotential-deposited H, which strongly commences at this potential just beyond 0.2 V on Pt(100) [Figure 1, ref 1], is opening up more sites for H_2 oxidation, and this is directly responsible for the current increase (we thank a reviewer for suggesting this speculative interpretation). It is further noted from Figure 1 in ref 1 that at about 0.45 V the upd H is removed and the electrode double layer region is entered. It may be seen that from 0.45 to 0.7 V, which is the range of the double layer region, H_2 oxidation current reaches a maximum that could be the diffusion limit. At greater than about 0.7 V the current begins to decrease, possibly because of site blocking by H_2O(ads) and its oxidation product OH(ads). This is all illustrated in Figure 4, which shows the full range of current measurements.

Conclusions

The fit of the theoretical Tafel plot, based on calculated activation energies for the Heyrovsky step, which is the rate-limiting first electron-transfer step in H_2 oxidation and the second step in H_2 evolution, to the experimental Tafel plot for Pt (100) electrodes gives strong support for the participation of the Volmer−Heyrovsky mechanism for the two-electron processes. On the basis of the fit, the Heyrovsky step is rate limiting. The theory does not support this mechanism over the (110) electrode and is ambiguous for the (111) electrode, in agreement with the conclusions of ref 1. This study illustrates that curvature in nonlinear Tafel plots may stem from the potential dependence of the activation energies or transfer coefficients as well as surface coverage, diffusion, and concentration gradient effects. A full understanding of these effects taken together is an experimental and theoretical challenge for the future. Finally, an interpretation is proposed for the whole Tafel plot, including previously unpublished data, wherein as the potential is increased from the activation energy-controlled region the kinetic current increases as upd H is removed until a limit is reached and in the double layer region and then decreases as water reacts with the surface and OH(ads) forms.

Acknowledgment. We thank Dr. Nenad Markovic for providing unpublished Tafel data. This research is supported by the National Science Foundation, Grant. No. CHE-9982179.

References and Notes

(1) Markovic, N. M.; Grgur, B. N.; Ross, P. N. *J. Phys. Chem. B* **1997**, *101*, 5405−5413.

(2) Gileadi, E *Electrode Kinetics for Chemists, Chemical Engineers, and Materials Scientists*; VCH Publishers: New York, 1993; p 130.

(3) Anderson, A. B.; Kang, D. B. *J. Phys Chem. A* **1998**, *102*, 5993−5996.

(4) Anderson, A. B.; Albu, T. V. *J. Electrochem. Soc.* **2000**, *147*, 4229−4238.

(5) Anderson, A. B.; Sidik, R. A.; Narayanasamy, J.; Shiller, P. *J. Phys. Chem. B* **2003**, *107*, 4618−4623.

(6) Cai, Yu; Anderson, A. B. *J. Phys. Chem. B* **2004**, *108*, 9829−9833.

(7) Gurney, R. W. *Proc. R. Soc.* **1931**, *A134*, 137−154.

(8) Marcus, R. A.; Sutin, N. *Biochim. Biophys. Acta* **1985**, *811*, 265−323.

(9) Conway, B. E.; Wilkinson, D. P. *Electrochim. Acta* **1993**, *38*, 997−1013.

(10) Frisch, M. J.; Trucks, G. W.; Schlegel, H. B.; Gill, P. M. W.; Johnson, B. G.; Robb, M. A.; Cheeseman, J. R.; Keith, T.; Petersson, G. A.; Montgomery, J. A.; Raghavachari, K.; Al-Laham, M. A.; Zakrzewski, V. G.; Ortiz, J. V.; Foresman, J. B.; Cioslowski, J.; Stefanov, B. B.; Nanayakkara, A.; Challacombe, M.; Peng, C. Y.; Ayala, P. Y.; Chen, W.; Wong, M. W.; Andres, J. L.; Replogle, E. S.; Gomperts, R.; Martin, R. L.; Fox, D. J.; Binkley, J. S.; Defrees, D. J.; Baker, J.; Stewart, J. P.; Head-Gordon, M.; Gonzalez, C.; Pople, J. A. *Gaussian 94*, revision C3; Gaussian, Inc.: Pittsburgh, PA, 1995.

(11) Kostadinov, L. N.; Anderson, A. B. *Electrochem. Solid State Lett.* **2003**, *6*, E30-E33.

(12) Bockris, J. O'M; Khan, S. U. M. *Surface Electrochemistry*; Plenum Press: New York, 1993; p 493.